Cerebral Cortex, January 2017;27: 750–763

doi:10.1093/cercor/bhv275
Advance Access Publication Date: 15 November 2015
Original Article

ORIGINAL ARTICLE

Spontaneously Emerging Patterns in Human Visual Cortex Reflect Responses to Naturalistic Sensory Stimuli

Meytal Wilf[1], Francesca Strappini[1], Tal Golan[2], Avital Hahamy[1], Michal Harel[1] and Rafael Malach[1]

[1]Department of Neurobiology, Weizmann Institute of Science, Rehovot 76100, Israel and [2]The Edmund and Lily Safra Center for Brain Sciences, Hebrew University of Jerusalem, Jerusalem, Israel

Address correspondence to Rafael Malach. Email:rafi.malach@weizmann.ac.il

Abstract

In the absence of stimulus or task, the cortex spontaneously generates rich and consistent functional connectivity patterns (termed resting state networks) which are evident even within individual cortical areas. We and others have previously hypothesized that habitual cortical network activations during daily life contribute to the shaping of these connectivity patterns. Here we tested this hypothesis by comparing, using blood oxygen level-dependent-functional magnetic resonance imaging, the connectivity patterns that spontaneously emerge during rest in retinotopic visual areas to the patterns generated by naturalistic visual stimuli (repeated movie segments). These were then compared with connectivity patterns produced by more standard retinotopic mapping stimuli (polar and eccentricity mapping). Our results reveal that the movie-driven patterns were significantly more similar to the spontaneously emerging patterns, compared with the connectivity patterns of either eccentricity or polar mapping stimuli. Intentional visual imagery of naturalistic stimuli was unlikely to underlie these results, since they were duplicated when participants were engaged in an auditory task. Our results suggest that the connectivity patterns that appear during rest better reflect naturalistic activations rather than controlled, artificially designed stimuli. The results are compatible with the hypothesis that the spontaneous connectivity patterns in human retinotopic areas reflect the statistics of cortical coactivations during natural vision.

Key words: beep detection, fMRI, movie, resting state, retinotopy

Introduction

In the absence of external stimulation or task, during what is termed "resting state," the human cerebral cortex generates ultra-slow spontaneous fluctuations that are robust and highly consistent (Fox and Raichle 2007). These spontaneous fluctuations have also been demonstrated to reflect ultra-slow modulations in firing rate (Nir et al. 2008) as well as in local field potential (Leopold et al. 2003; He et al. 2008; Nir et al. 2008), and were also found during sleep (Ramot et al. 2013) and anesthesia (Arieli et al. 1996). An important aspect of these spontaneous fluctuations is the tendency of cortical networks to fluctuate in tandem, generating a rich and highly informative correlation patterns (also termed "functional connectivity" patterns; Biswal et al. 1995), which have been extensively studied in recent years (e.g., Fox et al. 2005; Nir et al. 2006; Fox and Raichle 2007; He et al. 2008).

However, despite a large body of research, it is not fully established what is the information that is actually coded in these spontaneously emerging correlation patterns. It has been originally proposed that the correlation patterns reflect an intrinsic structure of large-scale networks that are activated during various tasks (Greicius and Menon 2004; Smith et al. 2009; Deco et al. 2011; Goñi et al. 2014). However, following the pioneering research of Kenet et al. (2003) in anesthetized animals, further studies begin to indicate that the spontaneous functional connectivity patterns can show exquisite patterning also within specific sensory systems, and even within individual cortical areas. Thus far, intraregional connectivity patterns have been

demonstrated within primate (Wang et al. 2013) and human (Long et al. 2014) somatosensory cortex, as well as within the primate auditory cortex (Fukushima et al. 2012).

A particularly convenient system to examine such patterns is the set of retinotopically organized areas in the human visual cortex. This is because any connectivity pattern that may be mapped to a visual region can also be projected onto the corresponding visual topographic coordinates. The findings of robust spontaneous fluctuations in the human visual cortex in the absence of sensory stimulation (Nir et al. 2006) led to a number of recent studies that have explored how the functional connectivity of these regions relates to the retinotopic organization of the visual cortex. Several studies found that visual regions with similar receptive-fields tend to fluctuate in a correlated manner (Heinzle et al. 2011; Butt et al. 2013; Gravel et al. 2014; Raemaekers et al. 2014). This was true regardless of areal borders, that is, even when the voxels were not of the same visual area (Buckner and Yeo 2014). Additionally, cross-hemispheric connections were found between homolog topographical locations within the visual cortex (Raemaekers et al. 2014). Moreover, the spontaneously formed connectivity patterns, especially in areas V1–V3, were found to follow eccentricity organization, including even regions with nonoverlapping receptive fields, but representing iso-eccentricity points (Yeo et al. 2011; Arcaro et al. 2015). While these studies offer potential principles that may underlie the organization of resting state connectivity in the human visual cortex, the processes that may underlie the emergence of these specific organizing principles rather than others remain unclear.

Recently, we and others have proposed that the spontaneous connectivity patterns are not the exclusive consequence of intrinsic anatomical structuring, but that, in addition, Hebbian-like shaping of the cortical connectivity patterns that occur during daily life may play an important role in their detailed organization. In other words, the connectivity patterns that appear during rest may actually constitute a record of habitual past cortical coactivations (Fiser et al. 2010; Harmelech and Malach 2013; Sadaghiani and Kleinschmidt 2013). A number of recent experimental results support this hypothesis. For example, it has been shown that the spontaneous connectivity patterns carry a long-term trace of prior training and activation patterns (Lewis et al. 2009; Tambini et al. 2010; Taubert et al. 2011; Harmelech et al. 2013). Similarly, the level of interhemispheric motor-cortex connections has been shown to reflect the habitual bimanual hand usage in congenital amputees (Hahamy, Sotiropoulos et al. 2015). In addition, aberrant task-evoked activation patterns in the visual system have been shown to be recapitulated in resting state functional connectivity (Gilaie-Dotan et al. 2013).

It occurred to us that the spontaneously emerging patterns in retinotopic visual areas could provide a powerful testing ground for the above-mentioned hypothesis. If indeed the spontaneous connectivity patterns in the visual cortex were shaped by the habitual coactivations produced by natural visual stimulation, then we would expect these patterns to be more similar to the patterns produced by naturalistic visual stimuli compared with the more controlled stimuli typically employed in visual experiments.

In the present study, we set out to examine whether the connectivity patterns evoked by laboratory-designed stimuli resemble those that emerge during resting state, and how these compare with the patterns evoked by a naturalistic stimulus. To that end, we directly compared resting state connectivity patterns with movie-driven ones and with patterns generated by stimuli optimal for retinotopic mapping. Our results reveal that the patterns of connectivity driven by free viewing of a movie segment showed significantly higher similarity to the resting state spontaneous connectivity patterns compared with other, artificial stimuli, including eccentricity mapping stimuli. Our results are thus compatible with the hypothesis that spontaneous connectivity patterns reflect the habitual cortical activations that occur during natural viewing conditions.

Materials and Methods

Experimental Procedure

Fourteen participants took part in 2 experimental sessions (mean ± SD age 28 ± 2 years, 5 males, 2 left handed); none had neurological or attentional disorders. Participants gave written informed consent prior to the experimental sessions and all procedures were approved by the Hertzog Hospital Ethics Committee.

In the main experimental session (Fig. 1A), participants were instructed to close their eyes and rest without thinking of anything in particular for 8 min (the session always began with a resting state period). Next, eight of the participants performed 2 runs of an 8-min beep detection task, in which they were instructed to press a button every time they heard a beep (pure tone, low volume beeps were played every 4–12 s). The stimuli presentation and button press recordings were implemented in Matlab using the Psychophysics Toolbox extensions (Brainard 1997; Pelli 1997). Additionally, participants freely viewed 2 repetitions of an 8-min segment of a naturalistic feature film in Hebrew ("Broken Wings"). The movie segment contained several highly emotional scenes, which included people conversing and using tools, and also contained music, and landscape shots. The movie segment was preceded by 15 s of blank screen and a 15-s visual adaptation stimulus (alternating colorful patterns). Only the 8-min movie segment was used for the analyses.

All participants underwent an additional session of standard retinotopic mapping. The order of the 2 sessions (main experimental session and retinotopic mapping session) was counterbalanced between participants. The retinotopic mapping session included 2 repetitions of a flickering black and white checkerboard rotating wedge stimulus ("polar angle"), and of an expanding ring stimulus (maximum diameter 17° of visual angle; "eccentricity"; Figure 1A; similar to Sereno et al. 1995). The stimuli were generated using a modified version of a Matlab program originally created by Dr Samuel Schwarzkopf (https://sampendu.wordpress.com/retinotopy-tutorial/). The duration of one complete polar angle or eccentricity cycle was 60 s; 8 cycles were presented during each functional magnetic resonance imaging (fMRI) run, to a total of 8 min. Participants were required to maintain fixation on a central dot, and press a button when the fixation changed its color to red (a rare event, meant to keep the participants alerted). This retinotopic mapping (polar angle and eccentricity) allowed us to define the boundaries of retinotopic cortical areas (V1, V2, V3) on the cortical surface for each individual participant on the basis of the visual field sign (Sereno et al. 1995).

Imaging Setup and fMRI Analysis

Images were acquired using a 3 Tesla scanner (Tim Trio, Siemens), equipped with a receive-only 12–channels head matrix coil. Functional T_2^*-weighted images were acquired with a gradient echo EPI sequence with a repetition time (TR) of 2000 ms, an echo time (TE) of 27 ms ,a 75° flip angle, a resolution of 3 × 3 × 3.3 mm, acquiring 34 transverse slices tilted to the anterior commissure–posterior commissure plane, covering the whole brain without gaps. Two 3D gradient echo T_1-weighted anatomical images were acquired to facilitate the incorporation and registration of

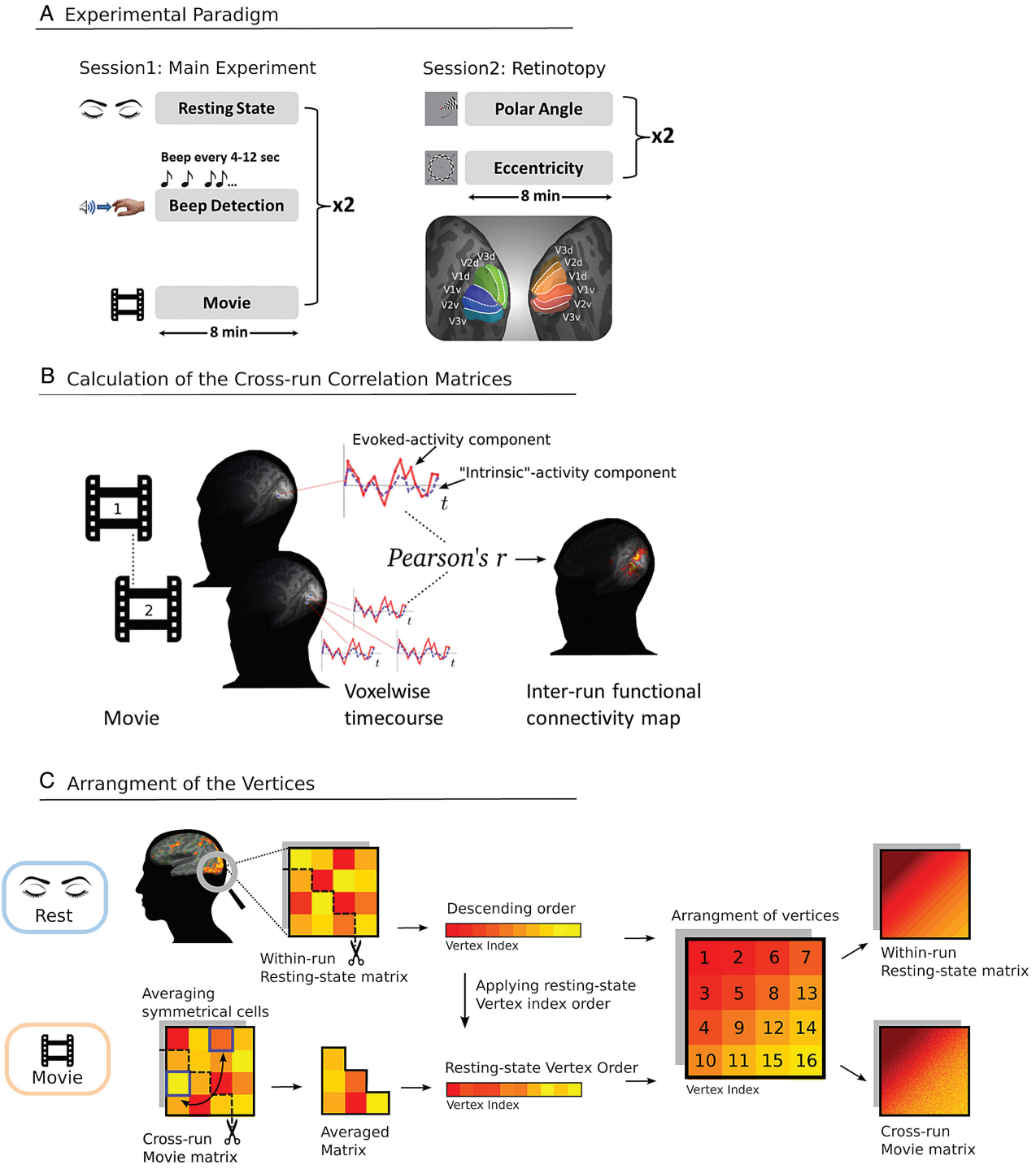

Figure 1. Experimental design and methodological approach. (*A*, left) The experiments in the main experimental session included resting state, auditory task, and free viewing of a movie segment. Note that each condition had 2 repetitions, and the session always began with resting state. (*A*, right) In the retinotopic mapping session each visual condition was presented twice. These stimuli were used to define retinotopic visual areas for each participant (see Materials and Methods). The order of the 2 sessions was counterbalanced between participants. (*B*) In order to avoid non stimulus-driven effects in analyzing visually induced conditions, an inter-run approach was used. Stimulus-driven functional connectivity was calculated by taking the seed voxel from one movie repetition and correlating it with all the other voxels in the other movie repetition (see Materials and Methods). (*C*) Schematic illustration of the sorting procedure of the correlation matrices according to the resting state correlations (see Materials and Methods).

the functional data into the 3D native anatomical space. The anatomical images were acquired with a resolution of 1 × 1 × 1 mm using the 3D-MPRAGE sequence with TR/TE/inversion time (TI)/flip angle of 2300 ms/2.98 ms/900 ms/9°. During preprocessing anatomical imaged were averaged in FreeSurfer to improve signal-to-noise ratio (Dale et al. 1999).

All fMRI data were processed using FSL 5.0.2.1 (www.fmrib.ox.ac.uk/fsl), FreeSurfer (Dale et al. 1999; Fischl et al. 1999;

http://surfer.nmr.mgh.harvard.edu/, last accessed November 5, 2015), AFNI, SUMA (Cox, 1996; http://afni.nimh.nih.gov/, last accessed November 5, 2015) and in-house Matlab code (Mathworks, Natick, MA, USA). Functional data were analyzed using FMRIB's expert analysis tool (FEAT, version 6). The following prestatistics processing was applied to the data of each individual participant: motion correction using FMRIB's Linear Image Registration Tool (MCFLIRT) (Jenkinson et al. 2002); brain extraction using BET (Smith et al. 2004); and high-pass temporal filtering with a cut-off frequency of 0.01 Hz. Functional images were aligned with high-resolution anatomical volumes initially using linear registration (FLIRT), then optimized using Boundary-Based Registration (Greve and Fischl 2009). The nonneuronal contributions to the BOLD signal were removed by linear regression of motion parameters, ventricle and white matter timecourses for each participant (Fox et al. 2009). The white matter and ventricles of each participant were automatically defined using FSL's FAST (Zhang et al. 2001), and manually refined to avoid boundaries between tissues (Hahamy, Behrmann et al. 2015). Global signal regression was not performed, as this procedure has been shown to distort connectivity patterns and remove potential neural signals (Murphy et al. 2009; Saad et al. 2012; Hahamy et al. 2014).

The cortical surface of each subject was reconstructed and inflated using FreeSurfer, based on the mean anatomical image of the 2 MPRAGE scans (Fischl et al. 1999; Fischl and Dale 2000). The individual surfaces of each subject were then imported to SUMA in subject space. Then the functional data were projected onto the native cortical surface of each participant using SUMA. Time courses were extracted from each vertex of each visual region defined by the retinotopic mapping.

Functional Connectivity Maps Within and Between Runs

A standard functional connectivity analysis was applied to the resting state condition: single voxels in the ventral part of regions V2 and V3 were each taken in turn as a seed (one-voxel seeds), and Pearson's correlation was calculated in Matlab between each seed voxel's timecourse and all the other cortical voxels' timecourses. The aim of the example functional connectivity figures was to visually illustrate the existence of long-range correlations between ventral to dorsal portions, and their change across conditions. Since the ventral and dorsal parts of V1 are adjacent in the cortex, seed voxels were only taken from the ventral parts of V2 and V3 to illustrate long-range connections. This procedure resulted in multiple maps with an r value for each voxel, from which one example map is depicted in Figure 2A. A functional connectivity map based on a single voxel as a seed was obtained for each of the 2 resting state runs. The map of the first resting state and the map of the second resting state were then averaged, to reduce the noise in the representation of the resting state correlation pattern. For visualization purposes only, prior to averaging, the maps were transformed into standard MNI space and the average map was back-transformed to native space. These transformations resulted in a better registration to the FreeSurfer surface without the excessive up-sampling that accompanies performing the Matlab calculations directly on the surface. The native map was then projected onto each participant's native inflated cortical surface.

For the visually driven conditions (movie viewing and retinotopic mapping) we chose not to perform a within-run functional connectivity analysis, in order to avoid effects on the correlation pattern which are not stimulus-driven (Golland et al. 2007; Hasson et al. 2010). Therefore, functional connectivity was calculated only between the 2 runs of each participant in the following manner: each seed voxel's timecourse was taken from the first movie presentation and was correlated with all the voxel timecourses of the second movie presentation (see Fig. 1B). The same procedure was then applied to the second versus first movie presentation, that is, each seed voxel's timecourse was taken now from the second movie presentation and was correlated with all the voxel timecourses of the first movie presentation. Thus for each seed voxel 2 maps were created, which were then averaged and projected onto FreeSurfer cortical surface using the same procedure described above.

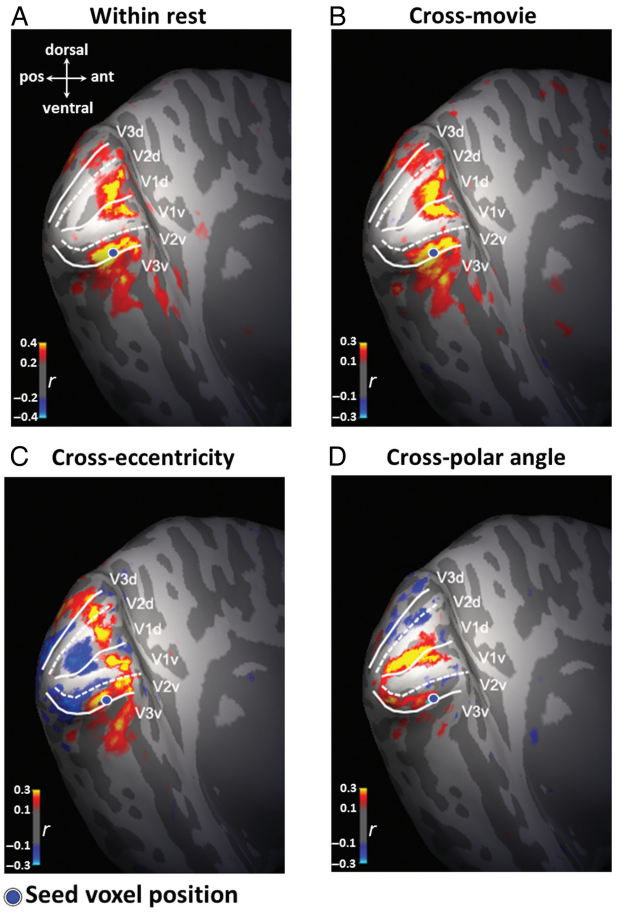

Figure 2. Example of the similarity between resting state and natural movie seed-based connectivity maps. Inflated representation of the posterior portion of the left hemisphere in a representative participant is presented, overlaid with a functional connectivity map of (*A*) Within resting state functional connectivity map with a seed voxel in ventral V2 (marked with a blue dot). Note the widespread correlations spanning the anterior section of up to dorsal V1 and V3. (*B*) Connectivity map between movie presentations (see Fig. 1*C*), using the same seed voxel. Note that the same patches arising spontaneously in the resting state map were driven coherently in this movie-driven map. (*C*) Connectivity map between eccentricity mapping repetitions using the same seed voxel. Note some similarity between the positive correlations in this map and the resting state correlations, as well as some anticorrelations (in blue) induced by the timing parameters of the visual stimulus. (*D*) Connectivity map between polar angle mapping repetitions using the same seed voxel. Here a different correlation pattern was generated with positive correlations mainly confined to the ventral visual areas, and negative correlation in the dorsal areas. V1–V3 borders are denoted by meridians lines (The dotted and solid lines indicate vertical and horizontal meridians, respectively). Maps were overlaid on the participant's native cortical surface (see Materials and Methods). Thresholds were chosen so as to equalize the number of positive voxels between maps, in order to emphasize similarity of correlation pattern and not strength. pos, posterior; ant, anterior.

Because we were interested in correlation patterns and not in overall correlation strengths, the thresholds of the maps presented in Figure 2 were chosen so that the maps contained similar number of positively correlated voxels (except for polar angle condition, which had a large spread of negatively correlated voxels, in which case the threshold was set according to the lowest threshold obtained from the other maps conditions).

Creating Area-Specific Vertex-by-Vertex Correlation Matrices

The complete pattern of correlations in each experimental condition within a given visual region (defined according to the retinotopic mapping run) was obtained as follows. The analysis examined areas V1, V2, V3 separately, either while joining together dorsal and ventral sections and both hemispheres (to a total of 2380 ± 151, 2581 ± 127, 2254 ± 89 vertices in V1, V2, V3 respectively), or by joining only the dorsal and ventral sections and keeping the hemispheres separated (1240 ± 80, 1337 ± 68, 1179 ± 62, 1140 ± 95, 1244 ± 75, 1075 ± 46 vertices in LH_V1, LH_V2, LH_V3, RH_V1, RH_V2, RH_V3, respectively). To obtain the full pairwise correlation matrix within each retinotopic area, the timecourses of all vertices within a retinotopic area (defined by the retinotopic mapping experiments) were extracted. Then, a pairwise Pearson's correlation matrix was calculated for all the vertices in each visual area. For experiments in which a visual stimulus was presented, the correlation of the vertices activity was calculated between and not within runs (the timecourses of all the vertices in the first stimulus presentation were correlated with the timecourses of all the vertices in the second stimulus presentation and vice versa; see "functional connectivity" section). This formed an asymmetrical matrix, such that the diagonal represented the timecourse correlation of the same vertex across the 2 stimuli presentations (similar to Golland et al. 2007). Values below the diagonal represented correlations of each of the seed vertices taken from the first stimuli presentation with all the vertices taken from the second stimuli presentation (and vice versa for values above the diagonal).

When no visual stimulus was presented (i.e., during resting state and beep detection runs), the correlation matrices were calculated within each run, and an average of the 2 within-run matrices was calculated to emphasize consistent correlation patterns, and reduce noise (forming a symmetrical matrix).

Creating Area-Specific Vertex-by-Vertex Distance Matrices

Five different topographic models were computed based on different types of distances between pairs of vertices: 1) Volume distance model: for each pair of vertices in the matrix the volumetric Euclidean distance in the 3D anatomical space was calculated to form a distances matrix, keeping the same vertex order as in the correlation matrices. 2) Surface distance model: in a similar manner, SUMA was used to calculate the shortest distance between each pair of vertices along the cortical surface. This analysis was only done for matrices containing vertices within a single hemisphere. 3) Polar angle distance model: the polar angle preference of each vertex was extracted based on the retinotopic mapping. Then the angular distance between each pair of vertices was calculated and assigned to its proper position in the matrix. 4) Eccentricity distance model: the eccentricity visual angle preference of each vertex was extracted based on the retinotopic mapping, and the angular distance of each pair was calculated. 5) Retinotopic location distance model: the preferred polar angle and eccentricity angle were combined for each vertex to create a single vector representing its preferred receptive field representation. These vectors were then used to compute the retinotopic distance between each pair of vertices.

Distances in all the models were inverted (1/ distance) so that close vertices would be represented by higher values, and farther away vertices would be represented by lower values.

Sorting Area-Specific Matrices According to Resting State Matrices

In order to better visualize the level of resemblance between the resting state and stimulus-driven connectivity patterns, the resting state correlation matrix of each visual area was sorted from strongest to weakest correlations in the following manner: since these matrices are symmetrical, only values below the diagonal were taken. These values were sorted according to their correlation strength, and were then arranged within a shape of a square so as to generate a salient pattern of correlation gradually moving from strongest to weakest values along a winding diagonal path (see Fig. 1C for demonstration). Critically, the index of the location of each value in the original resting state matrix was kept, so exactly the same index order could be applied to the stimulus-induced matrices as well (see Fig. 1C). Thus, the stimulus-induced and the distance matrices of each participant were rearranged not according to their own correlation strength, but according to the resting state matrix correlation strength. This ensured that if the original correlation pattern of a certain condition was similar to resting state, the new sorted square would present a gradual diagonal pattern similar to that of the corresponding resting state square.

In order to average the sorted squares across participants, the squares had to have similar dimensions. Because different participants had different original matrix sizes, the size of the mean square was determined by the smallest original matrix. Therefore, only a subset of the sorted correlation values was taken, to form for each participant a 1081 × 1081, 1371 × 1371, 1328 × 1328 size squares for V1, V2, V3, respectively. The squares were then averaged across participants and used for visualization.

Because the cross-run matrices were not symmetrical, values both below and above the diagonal had to be taken into account. This was done by averaging each value below the diagonal with its homolog value above the diagonal before creating the sorted square (i.e., the correlation of vertex *i* from the first run with vertex *j* from the second run was averaged with the correlation of vertex *j* from the first run with vertex *i* from the second run).

To better visualize the connectivity pattern regardless of overall correlation strength (which may differ between participants), the correlation values in each matrix were normalized by dividing each correlation value by the mean absolute value of the 2.5 and 97.5 percentiles (thus reducing the effect of the 5% outlier values on the matrix color range).

Correlation Between Spontaneous Connectivity Patterns and Stimulus Induced Patterns

For each participant, we examined the similarity between the resting state connectivity patterns (as well as patterns emerging during beep detection) and each of the stimulus-driven patterns. To that end, each unsorted matrix was transformed into a vector in the following manner: for the nonsymmetrical stimulus-driven matrices, the values below and above the diagonal were transformed into vectors, and then averaged (such that values were averaged symmetrically). For the averaged resting state

(and beep detection) matrices, only values below the diagonal were transformed into a vector as matrices were symmetric. The values along the main diagonal were disregarded in the comparison because the resting state diagonal is uninformative. The symmetrical distances matrices were also turned into a vector in a fashion similar to the resting state matrices. Then Pearson's correlation between the resting state vector and each of the stimulus-driven vectors was calculated for each participant separately in each region. For comparison between resting state vector and the different distance vectors, a nonparametric Spearman correlation was used (the correlation was done after the distances were inverted to 1/ distance).

All further statistical tests were performed after correlation values underwent Fisher's r to z transformation. One-sample *t*-tests were used to establish whether the correlations between the matrices of each condition and the resting state matrices were significantly greater than zero, and *P*-values were Bonferroni corrected (taking into account number of areas × number of conditions). Then, a 2-way repeated-measures analysis of variance (ANOVA) was performed taking visual area and condition as factors, to compare the level of similarity to resting state patterns between the different conditions, followed by Bonferroni corrected post hoc tests.

Controlling for Negative Correlations

We next aimed to eliminate the effect of negative correlations during retinotopy runs on the similarity between stimulus-driven matrices and resting state matrices. For this purpose, all negative values in the cross-run vectors of stimulus-evoked connectivity were transformed into zero before correlating them with the resting state connectivity vectors. Similar statistical tests were then applied on these nonnegative vectors, as previously described.

Plotting Average Cross-Run Correlations Against Binned Resting State Correlations

As a different way to visualize the relation between the resting state connectivity pattern and the stimulus-induced connectivity pattern, stimulus-induced connectivity values were plotted against resting state binned connectivity values in the following manner: vertex pairs were binned according to their resting state correlation, using 100 equally spaced bins (from $r = -1$ to $r = 1$) within each participant. Pairs with extreme correlation coefficients (top and bottom 99% and 1% of the values) were excluded from this analysis in order to reduce the effect of noisy or partially volumed voxels. The average cross-run correlation for each bin was calculated and plotted against each respective bin of resting state connectivity. An average line across participants was calculated for each experimental condition in each visual region, while considering only bins that were common to all participants.

The fit of each plot to a linear function was measured by a linear regression for each participant, and the R^2 value extracted in each experimental condition.

Reliability Measurement

A quantitative estimate of the reliability of our correlation patterns was obtained, to assess if indeed there was a stable stimulus-driven response between each 2 run repetitions. Note that for each pair of vertices we obtained 2 independent correlation measures—one value was obtained when we correlated the first voxel timecourse during the first stimulus presentation with the second voxel's timecourse during the second movie presentation. The second value was obtained by correlating the first voxel timecourse during the second movie presentation with the second voxel's timecourse during the first movie presentation. By comparing these 2 values we could get a measure of reliability of the overall correlation set. Thus, the vector of values below the diagonal was correlated with the vector of values above the diagonal to give the reliability measure for each matrix. A 2-way repeated-measures ANOVA was performed on the single-subject correlations taking visual area and condition as factors, followed by Bonferroni corrected post hoc tests.

Comparing Resting State Before and After the Movie Presentation

In an additional analysis, the original data from the 2 resting state periods were not averaged. Instead, after the matrices of the first and the second resting state periods were turned into vectors (as described above), the vectors were each correlated with the cross-movie vector separately.

Results

In the current study, we aimed to compare between spontaneously emerging connectivity patterns in the visual cortex and patterns that emerge during both naturalistic and laboratory-designed visual stimuli. Therefore, our experiment consisted of 2 resting state periods with eyes closed, and 2 repetitions of a naturalistic movie segment (14 participants). A subset of 8 participants performed an auditory beep detection task (Fig. 1*A*; see Materials and Methods). All participants also took part in an additional session for standard retinotopic mapping using 2 presentations of rotating wedge and expanding ring stimuli (see Fig. 1*A* and Materials and Methods).

In agreement with previous reports, examining the correlation patterns that emerged during rest with eyes closed revealed a wide spread and intricate pattern, that spanned long anatomical distances both within and across cortical areas. Figure 2*A* presents an example of seed-based correlations obtained from a single voxel's timecourse located in ventral area V2 (blue dot) while a participant rested in the scanner with eyes closed. As can be seen, the correlation to the seed voxel spanned well beyond its neighboring voxels in the anterior section of ventral V2, and reached as far as dorsal parts of V1 and V3, while forming a series of distinct patches in the anterior section of the primary visual areas.

Our goal was to compare the resting state correlation pattern to the pattern produced by each of the various visually induced conditions. Hence correlation maps from the same seed voxel were generated for each condition as depicted in Figure 2*B–D*. Panel 2B depicts the correlation of a single seed voxel timecourse during the first movie presentation with the timecourses of all other voxels during the second movie presentations, and vice versa (see Fig. 1*B* and Materials and Methods). It is important to emphasize that the correlation pattern calculated in this manner was strictly driven by the movie-stimulation and was not "contaminated" by the spontaneous signals that likely co-occur during the movie viewing. The timecourses of such spontaneous fluctuations were not phase-locked to the movie onset and did not share a common sequence and hence were not expected to show consistency across movie presentations. Panel 2C depicts the correlation pattern of the same seed voxel across repetitions of concentric ring stimulations ("eccentricity mapping", see Materials and Methods). Finally, Panel 2D depicts the same seed

correlation but across repetitions of a rotating wedge stimulation whose apex coincided with the fixation point ("polar angle mapping", see Materials and Methods). As evident, even by visual inspection, both the free viewing of the movie as well as the eccentricity mapping produced functional connectivity maps that were remarkably similar to the spontaneously emerging resting state functional connectivity. In contrast, the polar stimulation produced a correlation pattern that was only partially similar to the resting state one, mainly at short cortical distances.

To obtain the entire set of pairwise correlations during the various conditions, we calculated, separately for each area (V1–V3), a matrix of all pairwise vertex correlations (the correlations were calculated for all vertex pairwise combinations within each area including both dorsal and ventral parts in the 2 hemispheres). To allow a better visualization of the potential similarity between the patterns during the various conditions, the matrix cells were rearranged such as to show a gradient from high-to-low correlations during the resting state (see Fig. 1C and Materials and Methods). The indices (locations in the original matrix) of all cells in the rearranged resting state matrix were kept unchanged across all other conditions, but the values of correlations were replaced according to their values in each condition (see Fig. 1C and Materials and Methods). This allowed a direct visual comparison to the artificially sorted resting state matrices. It should be emphasized that this rearrangement of the resting state matrix is artificial and was conducted for visualization purposes only. The cross participant mean of these artificially constructed matrices can be seen in Figure 3A (see Materials and Methods). Note that similarity in correlation patterns between the resting state and other conditions should be revealed under this visualization scheme as a reappearance of the correlation gradient in the other conditions.

Figure 3B depicts the rearranged mean matrix of pairwise correlations driven by the movie stimulation. The movie-driven correlations were generated by taking the timecourse of one member of a vertex pair during movie 1 and correlating it with the timecourse of the second member of the pair during movie 2 and vice versa (see Materials and Methods and Fig. 1B,C), thus ensuring that the correlation will be driven by the movie and not "contaminated" by potentially ongoing spontaneous fluctuations. Although some degradation in the similarity to the resting state pattern can be discerned, the reemergence of the underlying structure is clearly evident. Panels 3C–3D depict the rearranged matrices of pairwise correlations for the correlation values, across repeats, of the eccentricity and polar angle stimuli. Both these conditions appear to show some traces of the resting state patterns, however, there was a marked reduction in similarity to the resting state pattern across all 3 retinotopic areas compared with the movie-driven correlation matrix. Note also that due to the nature of the retinotopic visual stimuli, a large extent of the pairwise correlations in these matrices were negative as opposed to the resting state and movie matrices. Finally, to assess the effect of the anatomical distance between vertices on the correlation pattern, the inverted Euclidean distance between each pair of vertices was measured (Fig. 3E; see Materials and Methods for details) and assigned to the rearranged matrix. As expected, as evident in Figure 3E, there was some contribution of anatomical distance to the resting state correlation pattern, but this effect could not account for the full richness of the resting state correlation pattern.

Next we quantified the similarity between resting state patterns and the stimulus-driven patterns under all other conditions (see Materials and Methods). Figure 4 depicts a summary histogram of the similarity between the connectivity patterns under the different conditions. The *Y* axis depicts how similar the stimulus-driven pairwise correlation pattern in each condition was to the pairwise correlation pattern during rest, separately for areas V1–V3. Two aspects can be discerned: First, all stimulus-driven visual correlations showed a significant similarity to the resting state pattern (smallest $t_{(13)} = 8.9$; $P < 0.001$ for all conditions ; one-sample *t*-test, Bonferroni corrected). Second, the movie-driven correlation pattern showed a significantly higher similarity to the resting state pattern compared with all other visual conditions. Overall, this similarity was significantly higher in V1 compared with the other regions (repeated-measures ANOVA showed $F_{2,26} = 5.04$, $P = 0.02$ for visual area; $F_{3,39} = 38$, $P = 0.000005$ for condition; and no interaction; post hoc tests show that the movie-driven correlations were more similar to rest compared with all other conditions $P < 0.0001$). As a control, we computed a correlation matrix between resting state periods, assuming no consistent pattern should emerge. Indeed, this cross-rest condition failed to show a significant similarity to the within-rest condition, in accordance with the spontaneous nature of the fluctuations in each of the resting state runs. These effects were not limited to the pattern of each area individually. Integrating the correlation matrix of areas V1–V3 into a single matrix (which included the cross-area correlations as well) showed an even more pronounced effect (see Supplementary Fig. 1; $F_{3,39} = 31.4$, $P = 0.00005$ for condition; movie higher than other conditions $P < 0.0005$, post hoc tests).

In addition, we have depicted the pairwise correlations between each of the cross-condition matrices and the resting state matrices in a line plot. In this plot, the *x* axis represented the resting state pairwise correlations (binned at 0.02 intervals), while the *y*-axis represented the pairwise correlations across conditions (see Supplementary Fig. 2). In this analysis, a better matching of the pattern of the matrices between rest and a condition should be expressed as a closer to linear function. Quantitative analysis in each of the cortical areas revealed that the cross-movie correlations showed a significantly more linear function compared with the cross-polar or eccentricity conditions ($P < 0.005$, $P < 0.05$, $P < 0.005$ for V1, V2, V3, respectively, *t*-tests on linear fit values, Bonferroni corrected). These results further confirm that the cross-movie correlations showed a significantly higher similarity to the resting state correlations.

However, as can be seen (Figs 2 and 3) the correlations during both the eccentricity mapping and polar mapping conditions included a substantial number of negative (anticorrelated) values, while the movie and the resting state correlations did not. To examine whether the existence of these negative values could explain the lower similarities between the retinotopic patterns and the resting state pattern, we repeated the analysis, but this time we replaced all negative values with zeros. Importantly, this manipulation did not substantially affect the results, (see Supplementary Fig. 3) and the correlation between the resting state patterns and movie patterns remained significantly higher than the correlations between the resting state patterns and any other condition ($P < 0.0001$, post hoc tests after repeated-measures ANOVA).

Additionally, to further examine the relative contributions of different topographic principles to the resting state patterns, the following analysis was performed (see Materials and Methods for more details): The preferred receptive field location of each cortical vertex was defined by the eccentricity and polar mapping results. Then an eccentricity model was constructed, which was inversely proportional to the visual field distance (in degrees of visual angle) between each 2 cortical vertices along the eccentricity dimension (i.e., ignoring changes along the polar dimension).

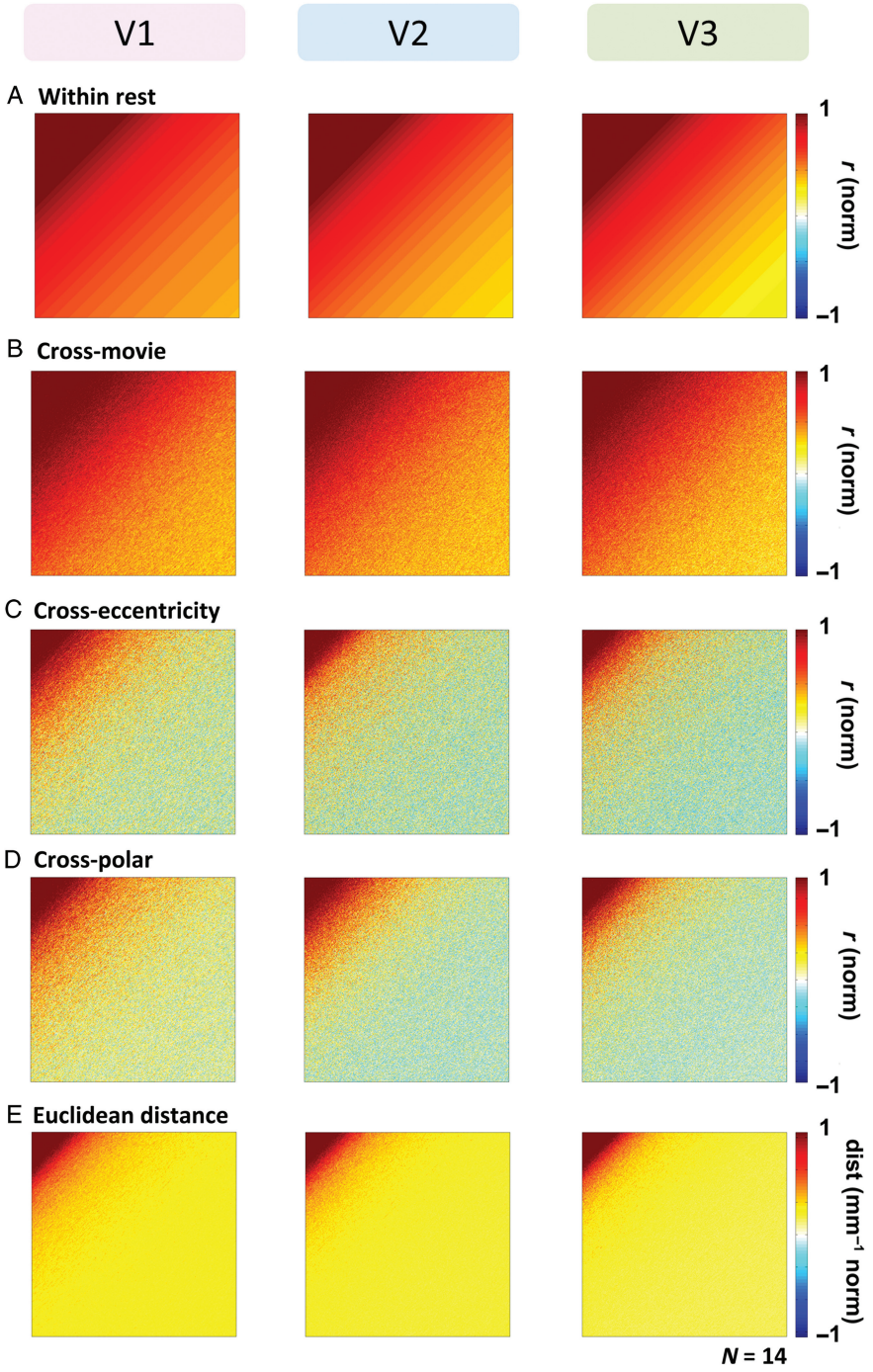

Figure 3. Similar resting state and movie patterns revealed in sorted mean correlation patterns of all vertices in each of the visual regions V1, V2, and V3. (*A*) The resting state pairwise correlation matrix of all vertices in a given visual area (V1, V2, V3) was sorted according to correlation strength to form a gradual pattern (see Materials and Methods). The mean matrix across all participants is presented ($N = 14$). (*B*) The same vertex order of the resting state matrix was kept but the pairwise correlation values were derived from the cross-movie matrix. The individual patterns were then averaged across participants. Note that the same gradual pattern reemerged in the naturalistic movie condition. (*C*,*D*) Same as *B*, but for eccentricity (*C*) and polar angle (*D*) conditions. Note that some similarity to resting state pattern remains, but it was less salient than that produced by the natural movie. Additionally, these conditions contain many negative correlation values. (*E*) Euclidean volumetric distance between each vertex pair (1/distance; high values represent nearby vertices). Values were normalized individually for each condition to demonstrate correlation pattern irrespective of amplitude (see Materials and Methods).

In a similar manner, a polar model in which the values were inversely proportional to visual field distances along the polar dimension was constructed. Finally, we constructed a retinotopic distance model, in which the values were inversely proportional to actual Euclidean visual field distance between the representations of each 2 cortical vertices. Note that these models did not contain any negative values, since the shortest possible distance between 2 vertices was zero. The results of this analysis are shown in Figure 5. Nonparametric statistics were used to get a measure of the ordinal correlation between the

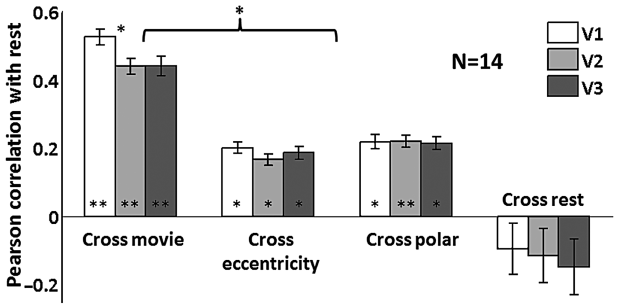

Figure 4. Naturalistic movie pattern shows significantly higher correlation to resting state pattern than other visual conditions. All visual conditions showed significant correlation to resting state, but the movie produced significantly higher correlations than all other visual conditions. Cross-resting state matrix failed to show a significant correlation to the within-run resting state patterns. Error bars denote standard error of the mean (±SEM); *$P < 0.05$ **$P < 0.000005$.

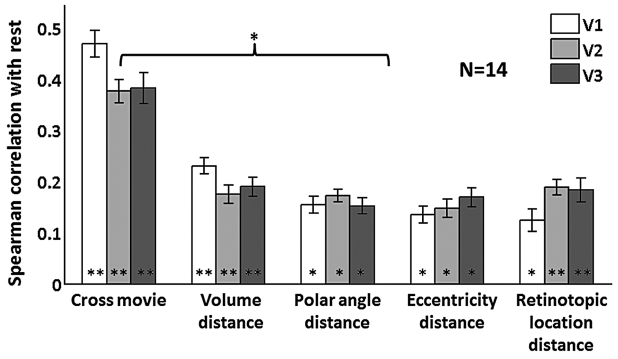

Figure 5. Movie pattern shows higher nonparametric correlation to resting state pattern than topographic distance models. Different models considering distances between vertex pairs in different retinotopic dimensions or distance in their location on the cortex were nonparametrically compared with the resting state pattern. Though all of the topographic principles contribute significantly to the resting state correlation, the movie still produces higher correlations to resting state. *$P < 0.0005$ **$P < 0.000005$.

resting state patterns and these topographic distance models. This way we could assess how well each of these models can predict the order of correlation strengths during resting state (assuming shorter distances in each of these dimensions would correspond to higher correlation during rest etc.). As can be seen, the cross-movie correlations were significantly higher compared with these model estimates, inferring that the strength order of correlations during resting state were better explained by the movie rather than by any of the topographic distance models ($P < 0.0005$, post hoc tests after repeated-measures ANOVA).

After obtaining the correlations between resting state patterns and the different retinotopic models with the 2 hemispheres combined, we next recalculated the correlations while considering the left and right hemisphere separately (see Materials and Methods). This enabled us to also generate a surface distance model of the correlation pattern. Figure 6 shows the ordinal correlation between resting state and movie pattern, as well as to the different distance models in each of the regions within the left and right hemisphere. This separate hemisphere analysis retained the same effect as the combined hemispheres analysis, and no difference between hemispheres was found ($F_{5,65} = 0.6$, $P = 0.6$ for area, repeated-measures ANOVA). In other words, the resting state correlation pattern was still more similar to the movie-evoked pattern than to all the other distance models. Additionally, conducting the analysis separately on the dorsal and ventral quarter-field representations of each visual areas, confirmed Arcaro et al. (2015) finding of a higher correlation for eccentricity coordinates compared with polar ones ($P = 0.13$, $P = 0.0003$, $P = 0.003$ for V1, V2, V3, respectively; post hoc tests after repeated-measures ANOVA).

It could also be argued that the reason that the movie-driven pattern showed higher similarity to the resting state pattern compared with the more artificial eccentricity and polar stimuli was a trivial consequence of reliability. If, for example, the eccentricity stimuli were less engaging, thus producing weaker and less reliable stimulus-driven signals—the consequent patterns generated by these stimuli will be noisier and hence show poorer similarity to the rest pattern. Note that only activity that is driven by the stimulus would contribute to the stimulus-driven matrices, because those matrices were based on cross-run correlations (see Materials and Methods). To examine this potential confound we calculated how reproducible was the pattern of correlation generated by each stimulus condition. This was obtained by simply measuring the similarity of the patterns when calculating them from 2 independent data sets that were obtained for each condition (see Materials and Methods).

Figure 7 depicts the reliability measures for the different conditions. As expected, all stimulus-driven conditions showed a significantly reliable pattern (smallest $t_{(13)} = 9.7$; $P > 0.0001$; one-sample t-test, Bonferroni corrected). No significant reliability was found across resting state repetitions when considering the inter-run correlation—again, as expected given the spontaneous nature of these fluctuations. Notably, the auditory control condition of beep detection with eyes closed did not show significant reliability between runs, suggesting that the visual cortex was indeed fluctuating spontaneously and did not respond in a consistent manner to the auditory stimuli, which occurred at identical timing in the 2 beep detection tasks.

Importantly, the reliability of the movie-driven correlations was significantly lower than that of the eccentricity and polar mapping conditions ($F_{3,39} = 226$ for condition; $P < 0.0005$ for all conditions and all visual areas; repeated-measures ANOVA with Bonferroni corrected post hoc tests), ruling out higher reliability for the movie condition as an explanation for its higher correlation to the resting state pattern.

Next we set out to examine whether the correlation between the movie-evoked and the rest patterns was related to the level of the reliability of the cross-movie pattern, assuming that a more reliable pattern would yield a less noisy representation of the correlation pattern and hence more similarity to the rest pattern. Indeed, when plotting cross-movie reliability versus cross-movie similarity to the rest pattern for each participant, we found a significant linear relationship between the 2 measures, that is, higher reliability values produced higher similarity to the rest pattern (Fig. 7B; $r = 0.67$, 0.7, 0.77 and $P = 0.02$, 0.02, 0.004 for V1, V2, V3 respectively; Pearson's correlation Bonferroni corrected). This implies that the measured similarity between the movie-driven and spontaneous (resting state) connectivity patterns was likely an underestimation of the true similarity.

To address the concern that during rest participants may have systematically engaged in visual imagery, we compared connectivity patterns in all the conditions to the within-run pattern of correlations that emerged when participants were asked to perform a nonvisual task (beep detection), performed with eyes closed (hit rate of 98.9%). The results of this analysis are depicted in Figure 8. When comparing the pairwise within-run correlation matrix of the beep detection task to the cross-run matrices of the stimulus-driven conditions, the correlations were essentially identical

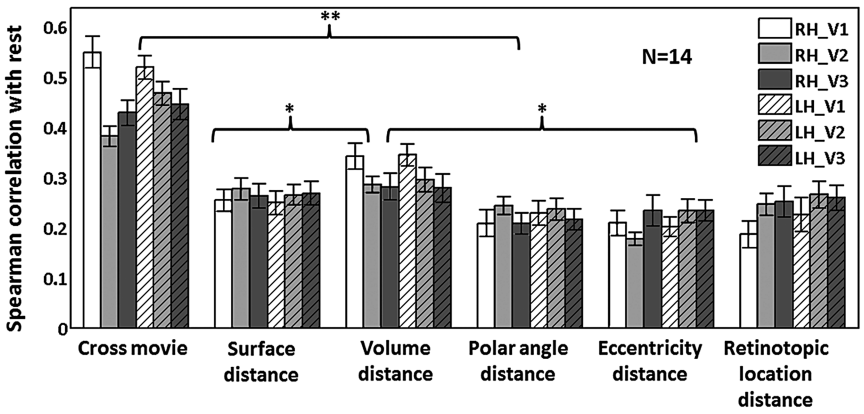

Figure 6. Comparing resting state pattern with topographic distance models while considering right and left hemispheres separately. All bars are significantly higher than zero, but movie is more similar to resting state than the other conditions. Volume distance model has higher correlations to resting state than the other distance models. RH, right hemisphere; LH, left hemisphere; *$P < 0.005$ **$P < 0.0005$.

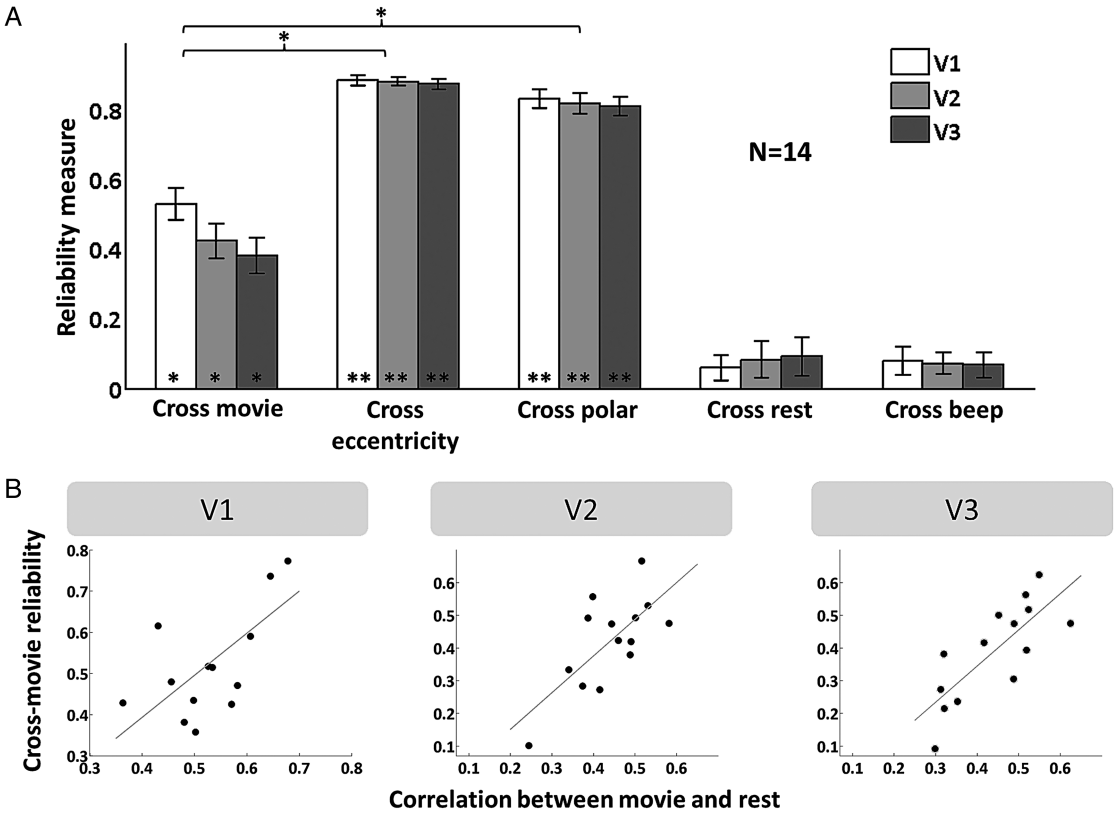

Figure 7. Eccentricity and polar angle conditions show higher reliability between runs than naturalistic movie. (*A*) The symmetry of the inter-run matrix in each condition was measured to assess reliability between runs (see Materials and Methods). Note that the movie patterns showed significant reliability between runs, albeit significantly lower than that of the better controlled eccentricity and polar angle stimuli. The nonvisual conditions (resting state and beep detection) showed no significant reliability in these primary visual areas. Error bars denote standard error of the mean (±SEM). (*B*) A scatter plot of reliability between movie runs versus the correlation of the cross-movie matrix to the resting state matrix in each individual participant (each dot denotes a participant). A linear relationship was found between these 2 measures. *$P < 0.05$ **$P < 0.00005$.

to those achieved with resting state ($N = 8$ for beep detection, and $N = 14$ for resting state; see Fig. 8). In fact, none of the correlations we tested showed any significant difference between resting state and beep detection (lowest P value was $P = 0.2$ for V1 cross-rest versus cross-beep, 2-sample t-test, Bonferroni corrected).

A direct comparison between within-run resting state and within-run beep detection patterns revealed a high similarity between these 2 nonvisual conditions (Fig. 8 leftmost bar). This high similarity can be appreciated also by noting the within-run beep matrices which were sorted according to resting state correlations (similar to Fig. 3; Supplementary Fig. 4).

In contrast, cross-run beep detection matrices showed close to zero correlations (average pairwise correlation, $\bar{r} = 0.01$, 0.004, 0.0007 in V1, V2, V3, respectively), in accordance with the spontaneous nature of fluctuations in visual cortex during this condition resulting in a very noisy pattern (see Supplementary Fig. 4C).

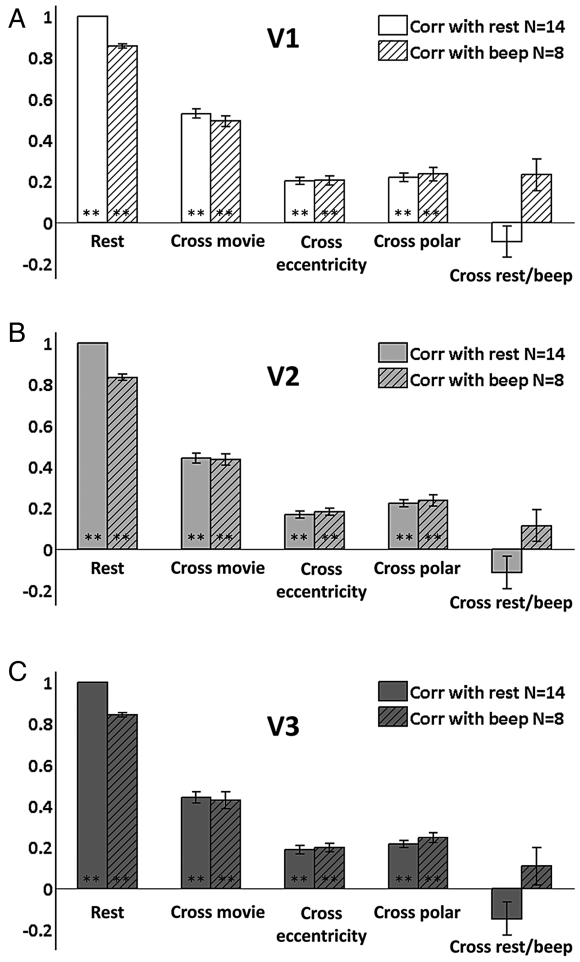

Figure 8. Within-run beep detection correlation pattern shows results very similar to resting state. (*A–C*) Direct comparison between within-run beep and within-run resting state correlations (leftmost bars) reveal a very high similarity. Recalculating pattern similarity to the different visual conditions using within-run beep detection instead of resting state show that none of the average correlations to beep detection were significantly different from correlations to resting state. Beep detection showed larger error bars, possibly due to smaller number of participants ($N = 8$).

Furthermore, the similarity of this cross-beep matrix and the resting state matrix was not significant ($W = 33$, 26, 24 and $P = 0.12$, 0.93, 1.2 for V1, V2, V3, respectively; $N = 8$; One-sampled Wilcoxon singed-rank test, Bonferroni corrected).

Finally, we examined any possible short term changes in resting state patterns that may have occurred between the first and second resting runs. To examine this, we compared the connectivity patterns of the resting state run acquired before participants watched the movie (the first rest), and those of the resting state run following the movie presentation (the second rest). This comparison revealed a small effect of higher similarity to the cross-movie pattern in the resting period following the movie ($F_{1,13} = 9.72$, $P = 0.008$; repeated-measures ANOVA). Importantly, even when considering only the pattern of the first resting state period (instead of the mean pattern of both the first and the second rest periods), it showed a significantly higher correlation to the cross-movie pattern than to the other visual conditions ($P < 0.0005$ in post hoc tests after repeated-measures ANOVA), ruling out a post-movie trace effect as the sole explanation for our results.

Discussion

Our study shows that the correlation patterns that emerge spontaneously in retinotopic visual cortex during resting state resemble those that are generated by naturalistic visual stimuli. The movie-driven patterns exhibited a significantly higher similarity to the spontaneous connectivity patterns compared with the patterns evoked by more conventional retinotopic mapping stimuli. Our study confirms and extends previous findings that support the notion that the resting state correlation patterns are not merely a reflection of large-scale anatomical networks, but show additional intricate patterning at finer detail, that is, within sensory systems and within individual visual areas as well. Specifically for the visual system, our study confirms the original findings of Nir et al. (2006) in showing wide spread correlation patterns, and further confirms previous studies showing long distance correlations within individual visual areas (Raemaekers et al. 2014; Arcaro et al. 2015).

Our results are also in-line with previous studies which convincingly demonstrated that the spontaneous connectivity patterns correlate with the center–periphery eccentricity organization across retinotopic visual areas (Yeo et al. 2011; Raemaekers et al. 2014; Arcaro et al. 2015). However, our results extend these previous results by demonstrating that free viewing of naturalistic sensory stimulation (a movie segment) produced patterns of correlations that were significantly closer to the resting state patterns compared with the patterns generated by either eccentricity-selective stimuli, polar-mapping stimuli, or merely anatomical distance (see Figs 4 and 5).

It is important to emphasize that the main focus of the present study was on the type of visual stimuli that may induce activations that best mimic the spontaneously emerging patterns. The space of such possible stimuli is obviously enormous and impossible to exhaust. We therefore opted to compare specifically 3 types of stimuli—2 types that are commonly used in retinotopic mapping experiments (eccentricity rings and polar wedges) and one that was aimed to simulate naturalistic vision. We also compared the movie-driven patterns to 5 putative organizational principles, in which the patterns followed eccentricity, polar, retinotopic location, surface distance, and volume distance. In all these comparisons, the cross-movie correlations proved to be significantly more correlated to the resting state patterns.

However, we acknowledge that we cannot rule out the possibility that additional stimuli of different kinds may produce patterns of activations that will show yet higher similarity to the spontaneous connectivity patterns. Nevertheless, even within this rather limited range of principles, our results are robust and informative as we discuss below.

Before discussing the implication of our findings, it is important to examine the potential confounds that could have contributed to the results. First, it could be argued that during the presumable "rest" participants were engaged in some kind of vivid visual imagery. Indeed, a major and general drawback of the resting state paradigm is that no control is exercised over the cognitive state of the participants when they are at rest. Here we controlled for this confound by asking the participants to engage in a nonvisual task (beep detection). The aim of the task was to prevent participants from intentionally choosing a strategy of engagement in visual imagery while they rested. However, it should be noted that the beep detection task was easy, so we cannot rule out the possibility that some visual imagery may have occurred during the beep detection performance. It could also be argued that even if the beep detection task was nonvisual, it may have significantly distorted the spontaneous functional connectivity patterns in the visual

cortex. However, several points argue against this possibility. First, previous research suggests that spontaneous activations may appear in nonactivated networks even when participants are engaged in a specific task (e.g., Golland et al. 2007). Second, the fluctuations in the visual system during the beep detection experiment exhibited low pattern reproducibility between the 2 beep detection periods (Fig. 7A), indicating that the visual cortex was not systematically driven by the beep stimuli or task but rather fluctuated spontaneously. This finding might be surprising in light of recent results reporting cross-modal audio-visual inhibition (Iurilli et al. 2012). However, the lack of task-related inhibition could derive from the fact that our task was not attentively demanding, and included sporadic stimuli. Therefore, at least in terms of the functional connectivity patterns, the fact that participants were engaged in an auditory beep detection task (with eyes closed), did not substantially disrupt the spontaneously emerging patterns in their visual cortex.

This result is significant in offering a potential solution to the more general problem of using the uncontrolled resting state paradigm. Thus, our results demonstrate that it is possible to employ controlled tasks even when examining spontaneous "resting state" connectivity patterns, as long as the networks under study are not driven by the task (see also Salomon et al. 2011).

A second confound that could produce higher similarities of the movie-driven patterns compared with the more artificial visual tasks patterns could be attentional and arousal effects. It could be argued that the artificial (wedges and rings) stimuli failed to engage the participants' attention, and consequently produced weaker and less reliable activations of the visual areas, leading to noisier cross-run correlation patterns. However, our reliability measures reveal that the contrary was true (Fig. 7A), that is, the artificial stimuli, probably due to the stricter control over stimuli and oculomotor behavior (imposed by fixation), produced more reliable activation patterns compared with the movie stimuli.

Finally, it could be argued that the similarity of the rest patterns to the movie-driven patterns reflected a direct trace of the specific movie shown to participants that is "replayed" in the spontaneous connectivity patterns, since half of the rest sessions were acquired after the movie was shown. Such immediate direct shaping of the spontaneous connectivity patterns by intense task activations has been reported previously (Hasson et al. 2009; Stevens et al. 2009; Tailby et al. 2015), and also at longer time scales (Harmelech et al. 2013). Indeed, when comparing the resting state patterns before and after participants watched the movie, we found a small but significant post-movie effect. However, at this stage we cannot determine whether this effect may have been due to training of the neuronal networks by the movie stimuli or was related to more general changes in arousal or attention associated with the second rest period. For example, correlation strength has been reported to increase during sleep (e.g., Nir et al. 2008). It may be that increased drowsiness has led to a similar increase in correlation strength which, due to a higher signal-to-noise ratio, could increase the correlation level during the second rest period. Importantly, the same effects found for the average of the 2 rest periods were fully replicated when only the first rest (recorded prior to any movie presentation) was used for the analysis. Thus, the data appear compatible with the notion that the high correlation found between movie-driven and resting state patterns was more related to some naturalistic parameters of the movie, rather than to a trace of the specific movie presented to the participants.

Thus, our results show that the naturalistic, free viewing conditions indeed induced visual activation patterns that were closely reflected in the patterns that emerged spontaneously in retinotopic visual areas, both during rest and during the auditory task. This is particularly remarkable because, as Figure 7 demonstrates, the naturalistic paradigm, lacking eye movement controls and specific tasks, substantially degraded the reliability of the movie-induced patterns. It is likely that under more reproducible conditions, such as repeating the movie several times (at long intervals), the correlations between the spontaneous and movie-driven patterns could become even higher. Thus, our results clearly demonstrate that the spontaneous, stimulus free patterns, while showing significant similarity to coactivations driven by conventional visual stimuli such as eccentricity and polar mapping, nevertheless contained additional details that were captured better by the naturalistic movie stimulus.

When comparing the connectivity patterns across the eccentricity and polar dimensions, it is important to note that within hemisphere, near neighbor interactions could be differentially pronounced in the polar than the eccentricity dimensions due to the interdigitated nature of vertical and horizontal meridian representations across visual areas. Thus, targeted analyses that focus on subdivisions within areas may emphasize different biases compared with the more global analysis approaches applied in the present study. Indeed analyzing separately the dorsal and ventral quarter-field representations confirmed Arcaro et al's (2015) finding of a preferential correlation to eccentricity compared with polar coordinates.

In the present study, we chose not to require participants to fixate while watching the movie, while resting, or while performing the nonvisual task. This might have reduced the reproducibility of cross-movie patterns, because the stimuli appearing on the retina were not necessarily similar between viewing periods. However, as we wished our experimental conditions to mimic natural vision as best as possible, we opted for the more ecological free viewing conditions. Additionally, resting state patterns with and without fixation have been shown to produce highly similar patterns (Fox et al. 2005; Fransson 2005; Arcaro et al. 2015).

The observed reflection of naturalistic movie patterns in the spontaneous connectivity patterns is nicely compatible with our proposed hypothesis (Harmelech and Malach 2013), that an important factor that shapes the resting state patterns is a Hebbian-like strengthening of functional connectivity, induced by habitual coactivations of cortical networks during daily life. Such coactivations presumably lead to synaptic changes that later modulate the correlation patterns appearing spontaneously during rest. Compatible with this suggestion, animal studies have shown that the similarity between naturalistic stimulation and spontaneous activity increases with development, while the similarity between nonnaturalistic (moving grating) visual stimuli and spontaneous activity does not (Berkes et al. 2011). Here we propose that habitual visual experience plays a role in shaping cortical connectivity during adult life as well.

While our results are compatible with the notion that the spontaneous connectivity patterns capture aspects of naturalistic vision, this does not rule out the possibility that important aspects of the spontaneous connectivity patterns are guided by intrinsic factors that are not necessarily experience-dependent. One such factor is, of course, anatomical distance, as previous research in primate visual cortex has emphasized the importance of short range anatomical connectivity in visual cortex (e.g., Amir et al. 1993). Indeed, in our analysis the spontaneous connectivity patterns were significantly contributed by neighboring interactions (see Fig. 5). Interestingly, recent studies have shown that the eccentricity and polar organization of the resting state patterns is not dependent on visual stimulation, by demonstrating its presence even in blind individuals (Bock et al. 2015; Striem-

Amit et al. 2015). Thus, a full account of the formation of spontaneous patterns should include intrinsic factors (that may be genetic or congenital) in combination with experience-dependent factors (that may be shaped by habitual network coactivations). Future research will be needed to parcel out the various contributions to these intriguing spontaneous connectivity patterns.

Because of the rich, multiscale, and diverse nature of naturalistic stimuli, it is extremely difficult to uncover the full set of organization principles and statistical tendencies that characterize them. Hence it is difficult to point out what aspect of the activations endowed the movie-driven patterns with their higher similarity to the spontaneous connectivity patterns compared, to, for example, the eccentricity-driven correlations. Future studies, moving gradually from highly controlled, schematic stimuli such as the eccentricity rings to more naturalistic stimuli could help in answering this question.

Finally, it is important to caution, that although our study shows a highly significant correlation between movie-driven patterns and the spontaneously emerging ones, this correlation does not prove causation. At this point, we cannot rule out the possibility that the movie stimuli simply activated a complex of intrinsically connected structures that also appear in the spontaneous fluctuations. Examining individuals that engage in drastically different visual environments in their daily life may provide important clues to this question. Thus, studying individuals with retinal abnormalities, those that work in artificial lighting conditions or are exposed to long periods of outdoor, peripheral visual stimuli, could further test the notion that the environment shapes the patterns of correlations that emerge spontaneously in the absence of visual stimulation.

Supplementary Material

Supplementary material can be found at: http://www.cercor.oxfordjournals.org/.

Funding

This study was supported by the EU FP7 VERE, EU HBP Flagship, ICORE ISF grants and the Helen and Martin Kimmel award to R.M.

Notes

Conflict of Interest: None declared.

References

Amir Y, Harel M, Malach R. 1993. Cortical hierarchy reflected in the organization of intrinsic connections in macaque monkey visual cortex. J Comp Neurol. 334:19–46.

Arcaro MJ, Honey CJ, Mruczek RE, Kastner S, Hasson U. 2015. Widespread correlation patterns of fMRI signal across visual cortex reflect eccentricity organization. eLife. 4:e03952.

Arieli A, Sterkin A, Grinvald A, Aertsen A. 1996. Dynamics of ongoing activity: explanation of the large variability in evoked cortical responses. Science. 273:1868–1871.

Berkes P, Orbán G, Lengyel M, Fiser J. 2011. Spontaneous cortical activity reveals hallmarks of an optimal internal model of the environment. Science. 331:83–87.

Biswal B, Zerrin Yetkin F, Haughton VM, Hyde JS. 1995. Functional connectivity in the motor cortex of resting human brain using echo-planar mri. Magn Reson Med. 34:537–541.

Bock AS, Binda P, Benson NC, Bridge H, Watkins KE, Fine I. 2015. Resting-state retinotopic organization in the absence of retinal input and visual experience. J Neurosci. 35:12366–12382.

Brainard DH. 1997. The psychophysics toolbox. Spatial Vis. 10:433–436.

Buckner RL, Yeo BT. 2014. Borders, map clusters, and supra-areal organization in visual cortex. NeuroImage. 93:292–297.

Butt OH, Benson NC, Datta R, Aguirre GK. 2013. The fine-scale functional correlation of striate cortex in sighted and blind people. J Neurosci. 33:16209–16219.

Dale AM, Fischl B, Sereno MI. 1999. Cortical surface-based analysis: I. segmentation and surface reconstruction. Neuroimage. 9:179–194.

Deco G, Jirsa VK, McIntosh AR. 2011. Emerging concepts for the dynamical organization of resting-state activity in the brain. Nat Rev Neurosci. 12:43–56.

Fischl B, Dale AM. 2000. Measuring the thickness of the human cerebral cortex from magnetic resonance images. Proc Natl Acad Sci. 97:11050–11055.

Fischl B, Sereno MI, Dale AM. 1999. Cortical surface-based analysis: II: Inflation, flattening, and a surface-based coordinate system. Neuroimage. 9:195–207.

Fiser J, Berkes P, Orbán G, Lengyel M. 2010. Statistically optimal perception and learning: from behavior to neural representations. Trends Cogn Sci. 14:119–130.

Fox MD, Raichle ME. 2007. Spontaneous fluctuations in brain activity observed with functional magnetic resonance imaging. Nat Rev Neurosci. 8:700–711.

Fox MD, Snyder AZ, Vincent JL, Corbetta M, Van Essen DC, Raichle ME. 2005. The human brain is intrinsically organized into dynamic, anticorrelated functional networks. Proc Natl Acad Sci U S A. 102:9673–9678.

Fox MD, Zhang D, Snyder AZ, Raichle ME. 2009. The global signal and observed anticorrelated resting state brain networks. J Neurophysiol. 101:3270–3283.

Fransson P. 2005. Spontaneous low-frequency BOLD signal fluctuations: an fMRI investigation of the resting-state default mode of brain function hypothesis. Hum Brain Mapp. 26:15–29.

Fukushima M, Saunders RC, Leopold DA, Mishkin M, Averbeck BB. 2012. Spontaneous high-gamma band activity reflects functional organization of auditory cortex in the awake macaque. Neuron. 74:899–910.

Gilaie-Dotan S, Hahamy-Dubossarsky A, Nir Y, Berkovich-Ohana A, Bentin S, Malach R. 2013. Resting state functional connectivity reflects abnormal task-activated patterns in a developmental object agnosic. Neuroimage. 70:189–198.

Golland Y, Bentin S, Gelbard H, Benjamini Y, Heller R, Nir Y, Hasson U, Malach R. 2007. Extrinsic and intrinsic systems in the posterior cortex of the human brain revealed during natural sensory stimulation. Cereb Cortex. 17:766–777.

Goñi J, van den Heuvel MP, Avena-Koenigsberger A, de Mendizabal NV, Betzel RF, Griffa A, Hagmann P, Corominas-Murtra B, Thiran J-P, Sporns O. 2014. Resting-brain functional connectivity predicted by analytic measures of network communication. Proc Natl Acad Sci. 111:833–838.

Gravel N, Harvey B, Nordhjem B, Haak KV, Dumoulin SO, Renken R, Ćurčić-Blake B, Cornelissen FW. 2014. Cortical connective field estimates from resting state fMRI activity. Front Neurosci. 8:339.

Greicius MD, Menon V. 2004. Default-mode activity during a passive sensory task: uncoupled from deactivation but impacting activation. J Cogn Neurosci. 16:1484–1492.

Greve DN, Fischl B. 2009. Accurate and robust brain image alignment using boundary-based registration. Neuroimage. 48:63–72.

Hahamy A, Behrmann M, Malach R. 2015. The idiosyncratic brain: distortion of spontaneous connectivity patterns in autism spectrum disorder. Nat Neurosci. 18:302–309.

Hahamy A, Calhoun V, Pearlson G, Harel M, Stern N, Attar F, Malach R, Salomon R. 2014. Save the global: global signal connectivity as a tool for studying clinical populations with functional magnetic resonance imaging. Brain Connectivity. 4:395–403.

Hahamy A, Sotiropoulos SN, Slater DH, Malach R, Johansen-Berg H, Makin TR. 2015. Normalisation of brain connectivity through compensatory behaviour, despite congenital hand absence. eLife. 4:e04605.

Harmelech T, Malach R. 2013. Neurocognitive biases and the patterns of spontaneous correlations in the human cortex. Trends Cogn Sci. 17:606–615.

Harmelech T, Preminger S, Wertman E, Malach R. 2013. The day-after effect: long term, Hebbian-like restructuring of resting-state fMRI patterns induced by a single epoch of cortical activation. J Neurosci. 33:9488–9497.

Hasson U, Malach R, Heeger DJ. 2010. Reliability of cortical activity during natural stimulation. Trends Cogn Sci. 14:40–48.

Hasson U, Nusbaum HC, Small SL. 2009. Task-dependent organization of brain regions active during rest. Proc Natl Acad Sci. 106:10841–10846.

He BJ, Snyder AZ, Zempel JM, Smyth MD, Raichle ME. 2008. Electrophysiological correlates of the brain's intrinsic large-scale functional architecture. Proc Natl Acad Sci. 105:16039–16044.

Heinzle J, Kahnt T, Haynes J-D. 2011. Topographically specific functional connectivity between visual field maps in the human brain. Neuroimage. 56:1426–1436.

Iurilli G, Ghezzi D, Olcese U, Lassi G, Nazzaro C, Tonini R, Tucci V, Benfenati F, Medini P. 2012. Sound-driven synaptic inhibition in primary visual cortex. Neuron. 73:814–828.

Jenkinson M, Bannister P, Brady M, Smith S. 2002. Improved optimization for the robust and accurate linear registration and motion correction of brain images. Neuroimage. 17:825–841.

Kenet T, Bibitchkov D, Tsodyks M, Grinvald A, Arieli A. 2003. Spontaneously emerging cortical representations of visual attributes. Nature. 425:954–956.

Leopold DA, Murayama Y, Logothetis NK. 2003. Very slow activity fluctuations in monkey visual cortex: implications for functional brain imaging. Cereb Cortex. 13:422–433.

Lewis CM, Baldassarre A, Committeri G, Romani GL, Corbetta M. 2009. Learning sculpts the spontaneous activity of the resting human brain. Proc Natl Acad Sci. 106:17558–17563.

Long X, Goltz D, Margulies DS, Nierhaus T, Villringer A. 2014. Functional connectivity-based parcellation of the human sensorimotor cortex. Eur J Neurosci. 39:1332–1342.

Murphy K, Birn RM, Handwerker DA, Jones TB, Bandettini PA. 2009. The impact of global signal regression on resting state correlations: are anti-correlated networks introduced? Neuroimage. 44:893–905.

Nir Y, Hasson U, Levy I, Yeshurun Y, Malach R. 2006. Widespread functional connectivity and fMRI fluctuations in human visual cortex in the absence of visual stimulation. Neuroimage. 30:1313–1324.

Nir Y, Mukamel R, Dinstein I, Privman E, Harel M, Fisch L, Gelbard-Sagiv H, Kipervasser S, Andelman F, Neufeld MY, et al. 2008. Interhemispheric correlations of slow spontaneous neuronal fluctuations revealed in human sensory cortex. Nat Neurosci. 11:1100–1108.

Pelli DG. 1997. The VideoToolbox software for visual psychophysics: transforming numbers into movies. Spat Vis. 10:437–442.

Raemaekers M, Schellekens W, van Wezel RJ, Petridou N, Kristo G, Ramsey NF. 2014. Patterns of resting state connectivity in human primary visual cortical areas: a 7T fMRI study. Neuroimage. 84:911–921.

Ramot M, Fisch L, Davidesco I, Harel M, Kipervasser S, Andelman F, Neufeld MY, Kramer U, Fried I, Malach R. 2013. Emergence of sensory patterns during sleep highlights differential dynamics of REM and non-REM sleep stages. J Neurosci. 33:14715–14728.

Saad ZS, Gotts SJ, Murphy K, Chen G, Jo HJ, Martin A, Cox RW. 2012. Trouble at rest: how correlation patterns and group differences become distorted after global signal regression. Brain Connectivity. 2:25–32.

Sadaghiani S, Kleinschmidt A. 2013. Functional interactions between intrinsic brain activity and behavior. NeuroImage. 80:379–386.

Salomon R, Bleich-Cohen M, Hahamy-Dubossarsky A, Dinstien I, Weizman R, Poyurovsky M, Kupchik M, Kotler M, Hendler T, Malach R. 2011. Global functional connectivity deficits in schizophrenia depend on behavioral state. J Neurosci. 31:12972–12981.

Sereno MI, Dale A, Reppas J, Kwong K, Belliveau J, Brady T, Rosen B, Tootell R. 1995. Borders of multiple visual areas in humans revealed by functional magnetic resonance imaging. Science. 268:889–893.

Smith SM, Fox PT, Miller KL, Glahn DC, Fox PM, Mackay CE, Filippini N, Watkins KE, Toro R, Laird AR. 2009. Correspondence of the brain's functional architecture during activation and rest. Proc Natl Acad Sci. 106:13040–13045.

Smith SM, Jenkinson M, Woolrich MW, Beckmann CF, Behrens TE, Johansen-Berg H, Bannister PR, De Luca M, Drobnjak I, Flitney DE. 2004. Advances in functional and structural MR image analysis and implementation as FSL. Neuroimage. 23: S208–S219.

Stevens WD, Buckner RL, Schacter DL. 2009. Correlated low-frequency BOLD fluctuations in the resting human brain are modulated by recent experience in category-preferential visual regions. Cereb Cortex. 20:1997–2006.

Striem-Amit E, Ovadia-Caro S, Caramazza A, Margulies DS, Villringer A, Amedi A. 2015. Functional connectivity of visual cortex in the blind follows retinotopic organization principles. Brain. 138:1679–1695.

Tailby C, Masterton RA, Huang JY, Jackson GD, Abbott DF. 2015. Resting state functional connectivity changes induced by prior brain state are not network specific. NeuroImage. 106:428–440.

Tambini A, Ketz N, Davachi L. 2010. Enhanced brain correlations during rest are related to memory for recent experiences. Neuron. 65:280–290.

Taubert M, Lohmann G, Margulies DS, Villringer A, Ragert P. 2011. Long-term effects of motor training on resting-state networks and underlying brain structure. Neuroimage. 57:1492–1498.

Wang Z, Chen LM, Négyessy L, Friedman RM, Mishra A, Gore JC, Roe AW. 2013. The relationship of anatomical and functional connectivity to resting-state connectivity in primate somatosensory cortex. Neuron. 78:1116–1126.

Yeo BT, Krienen FM, Sepulcre J, Sabuncu MR, Lashkari D, Hollinshead M, Roffman JL, Smoller JW, Zöllei L, Polimeni JR. 2011. The organization of the human cerebral cortex estimated by intrinsic functional connectivity. J Neurophysiol. 106:1125–1165.

Zhang Y, Brady M, Smith S. 2001. Segmentation of brain MR images through a hidden Markov random field model and the expectation-maximization algorithm. IEEE Trans Med Imaging. 20:45–57.